

## Diffuse emission of $\gamma$ -ray and $\nu$ fluxes at very high energy and the Galactic/extragalactic cosmic ray transition

Silvia Vernetto<sup>a,\*</sup> and Paolo Lipari<sup>b</sup>

<sup>a</sup>INAF-OATO and INFN Sezione Torino, via P.Giuria 1, 10125 Torino, Italy

<sup>b</sup>INFN Sezione Roma “Sapienza”, piazzale A.Moro 2, 00185 Roma, Italy

E-mail: [vernetto@to.infn.it](mailto:vernetto@to.infn.it), [paolo.lipari@roma1.infn.it](mailto:paolo.lipari@roma1.infn.it)

Cosmic rays propagating in interstellar space in the volume of the Milky Way interact with gas and radiation fields generating gamma ray and neutrino emissions of comparable intensity. These emissions result in diffuse fluxes of secondary particles at the Earth that encode information on the space distribution, energy spectra and mass composition of the parent CRs in the entire volume of the Galaxy, where direct detection is not possible. Extending the measurements of the diffuse gamma ray flux to very high energy ( $> 100$  TeV) and detecting a neutrino flux above the atmospheric foreground is of great importance for our understanding of cosmic ray acceleration in Galactic sources and of the magnetic structure of the Milky Way.

The study of gamma rays and neutrinos in the energy range 100 TeV-10 PeV is of particular importance because their parent particles are around the prominent spectral feature known as the “knee”. The absorption probability for gamma rays in the PeV energy range distorts the energy and angular distributions of the diffuse flux, but taking into account these effects it is possible to obtain very valuable information also at these energies. In this work, starting from the CR data by direct measurements and air shower arrays, and using our model for the diffuse emission of gamma rays, we present predictions of the  $\gamma$ -ray flux under different hypothesis on the CR spatial and spectral distribution in the Galaxy, and compare our evaluations with the measurements in the 10 GeV-1 PeV energy range.

A second point of central importance that is addressed in this paper, is the identification of the transition energy where the contribution of extragalactic cosmic rays becomes dominant. All CR particles, of both Galactic and extragalactic origin, contribute to the diffuse  $\gamma$ -ray and  $\nu$  fluxes, but the two CR components are expected to have different space distributions and will generate diffuse fluxes that have angular distributions of different shape. This opens the possibility to identify or constrain the Galactic to extragalactic transition with observations of the  $\gamma$ -ray and  $\nu$  diffuse fluxes. This program requires to extend the measurements of the gamma ray diffuse flux to the 10–100 PeV energy range.

37<sup>th</sup> International Cosmic Ray Conference (ICRC 2021)

July 12th – 23rd, 2021. Online – Berlin, Germany

---

\*Presenter

## 1. Introduction

The main motivation for the study of the Galactic diffuse flux of gamma rays and neutrino is to understand (and measure) the space dependence of the CR populations in the Galaxy. This space distribution depends on the properties of the CR accelerators, and on the properties of CR propagation. In several models the space and energy dependences of the CR spectra are in good approximation factorized, i.e. the spectra have the same shape in all the Galaxy. This factorization is realized if the CR propagation is described by isotropic diffusion with a coefficient that has the same rigidity dependence in the entire volume of the Galaxy and if the CR sources can be considered (after appropriate averaging) as stationary and emitting a spectrum that does not depend on the space coordinates. This assumption has the immediate and important implication that, if absorption can be neglected the angular distribution of diffuse  $\gamma$ -ray and  $\nu$  fluxes are energy independent.

Observations of gamma rays by the Fermi telescope [1] are consistent with this hypothesis (within uncertainties), and the observed angular distribution, according to our previous study [2], implies that the CR density in the Galactic plane falls exponentially approximately  $\propto e^{-r/R}$  with a characteristic length  $R \sim 5$  Kpc ( $r$  is the distance from the Galactic center).

Some studies of the diffuse flux have however suggested [3, 4] that the factorization is violated, and that the CR spectra near the Galactic center have a harder spectrum than CR near the Sun. This possibility can be explored extending the range of observations of the diffuse flux to higher energy, to study experimentally the validity of the factorization (see discussion in [2]).

In Section 2 we will address this question, comparing the predictions of our diffuse emission model, obtained under different assumptions of CR spectral and space distribution, with the existing data, in particular the recent results by the Tibet ASy array above 100 TeV [5].

An other important open question that can be investigated with the study of the angular distribution of CRs, is the identification of the transition energy where the contribution of extragalactic cosmic rays becomes dominant. Extragalactic CR are expected to have a different spatial distribution with respect to Galactic CR and will produce gamma rays and neutrinos with a different angular distribution. In Section 3 we will evaluate the gamma ray and neutrino diffuse fluxes under different hypothesis on the Galactic/extragalactic origin of cosmic rays of energy above 100 PeV.

The prediction of the diffuse  $\gamma$ -ray and  $\nu$  fluxes requires the following elements: (1) a model for the CR spectra in all points in the Galaxy; (2) a model of the distributions of gas and radiation in interstellar space (gas and soft photons are the target for the interactions of CR particles, and the radiation fields also determine the gamma ray absorption probability); (3) a description of the interactions that generate  $\gamma$ 's and  $\nu$ 's.

In the following discussion we will use for (2) and (3) the models discussed in [2] (where gamma ray absorption is described according to [6]), limiting the discussion to point (1), namely the CR energy and space distributions.

## 2. The knee region and diffuse gamma rays

The CR energy spectra can be directly measured at the Earth, at low energy observing directly the primary particles with detectors on high altitude balloons or satellites, and at higher energy ( $E \gtrsim 10$  TeV) with extensive air shower (EAS) observations. The EAS measurements unfortunately

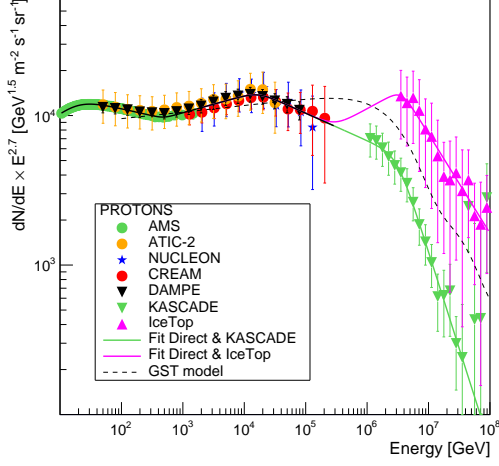


**Figure 1:** Proton spectrum according to direct measurements below 1 PeV, and by IceTop and KASCADE above 1 PeV, together with our best fit curves. The Gaisser-Stanev-Tilav model H3a (GST) [10] is also shown.

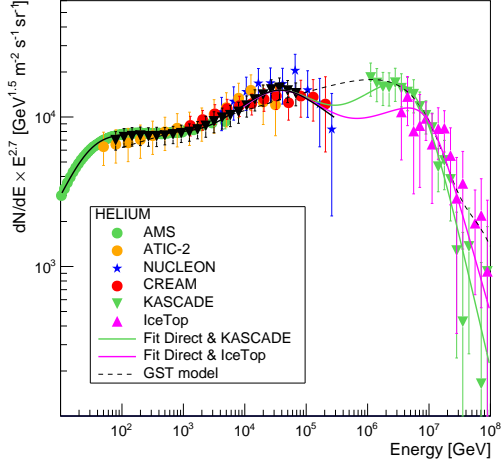


**Figure 2:** The same as Fig.1 but for helium nuclei. In both figures the error bars represent the quadratic sum of statistic and systematic errors.

have a poor mass resolution, and also suffer of large (and poorly understood) systematic errors associated to the description of hadronic interactions. The diffuse  $\gamma$ -ray and  $\nu$  fluxes, in good approximation, depends only on the “all-nucleon spectrum”, that gives the total flux of nucleons at the same energy per nucleon  $E_0$ , summing over the contributions of all nuclei. Uncertainties in the CR composition unfortunately however result in a quite large error in the estimate of the all-nucleon flux, and therefore also on the predictions of the diffuse fluxes.

In the last years direct measurements of the proton and helium fluxes have been performed by several instruments, covering the energy range from  $\sim 1$  GeV to  $\sim 200$  TeV. For both protons and helium nuclei two spectral features are evident: a hardening at a few hundreds GV rigidity, and a softening at  $\sim 10$ -20 TV. Above 100 TeV, the results by EAS arrays are much more controversial. We consider here the data of three ground based experiments: KASCADE, IceTop-IceCube and ARGO-YBJ. The IceTop proton spectrum [7] shows a flux much higher than that measured by KASCADE [8] with a knee at higher energy (Fig. 1), while for helium nuclei their data are relatively more consistent (Fig. 2). On the other hand, ARGO-YBJ measured the sum of proton and helium fluxes [9], detecting a knee at an energy well below 1 PeV, much lower than the values reported by the other experiments (Fig. 3). It is interesting to note that the connection of EAS spectra with direct measurements requires in general the presence of a further spectral hardening. To describe the whole spectra from 10 GeV to 100 PeV, we fit all the data with a function consisting of several power laws connected by breaks, an extension of the formula (1) given in [11].

Since at higher energy the data on heavy elements ( $Z > 2$ ) have even larger uncertainties, we estimated their flux by making the difference between the all-particle flux and the proton plus helium flux. The all-particle data used here and the best fit curve are shown in Fig. 3. Since the elemental composition of heavy nuclei is unknown, two extreme assumptions have been done: all heavy elements are a) Carbon, b) Iron. The obtained all-nucleon spectra (S1, S2, S3), derived by

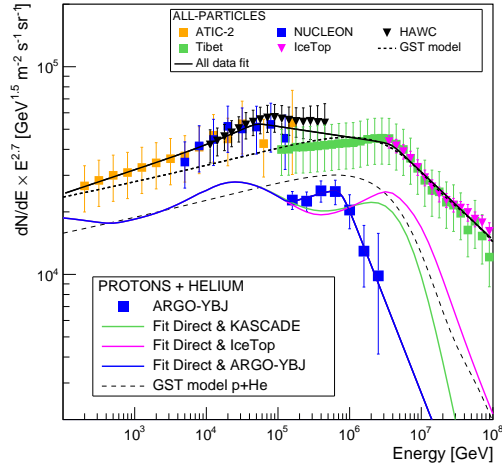


**Figure 3:** Spectrum of p+He nuclei, according to ARGO-YBJ data, with the relative best fit curve, compared to the sum of p+He best fit curves obtained from KASCADE and IceTop data. The all-particle spectra by different experiments and the corresponding best fit curve are also shown.

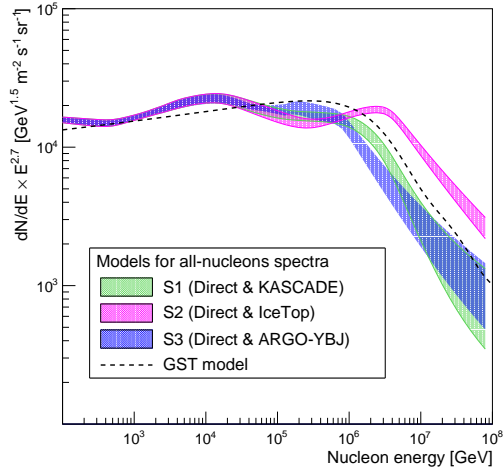


**Figure 4:** All-nucleon spectra obtained by using the p+He data of direct measurements and three EAS arrays.

the p+He data from the direct measurements and the three EAS arrays considered here, are shown in Fig. 4, where they are represented by a band with the lower limit corresponding to the Iron assumption and the higher limit to the Carbon one.

Given the local all-nucleon spectrum, the next step is the modeling of the spectrum in the whole Galaxy. We follow the approach described in [2], in which two different models of CR spectral distribution are considered. The first one (M1) assumes that cosmic rays have the same

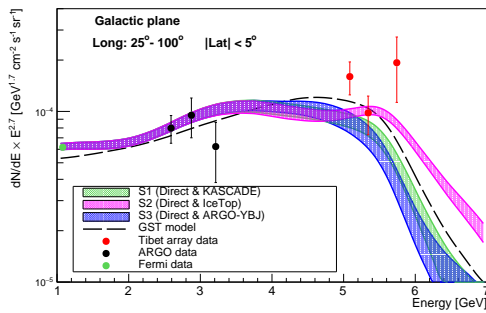


**Figure 5:** Diffuse gamma ray flux measured by the Tibet ASy array, ARGO-YBJ [12] and Fermi at 12 GeV [13], in a region of the Galactic plane, compared to the expectations of model M1 (that assumes the same CR spectral shape in all the Galaxy), for three local all-nucleon spectra (S1-S3)

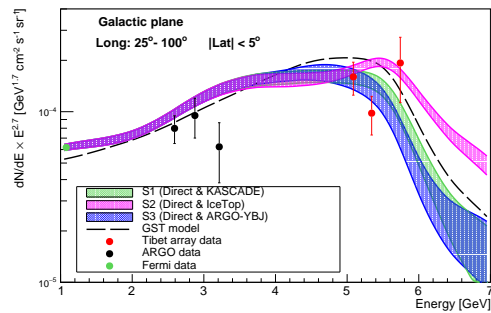


**Figure 6:** As Fig. 5, but using our model M2 for the CR spectral distribution in the Galaxy, that assumes a hardening of CR spectra towards the Galactic center (see details in [2])

spectral shape in the whole Galaxy, with an intensity decreasing according to  $\propto \text{sech}(r/R_c)$ , with  $R_c=5.1$  kpc ( $R_c$  has been obtained by fitting the Fermi longitudinal distribution of gamma rays of energy 12 GeV). The second model (M2) makes the further assumption that the CR spectra harden approaching the Galactic Center, according to [3, 4]. This hardening would produce a significant enhancement of the gamma ray flux of energy  $> 100$  TeV at smaller Galactic longitudes.

On these basis, we evaluate the expected gamma ray flux in the energy range 10 GeV-100 PeV, according to M1 and M2, for the three local spectra S1-S3. Fig. 5 and 6 show the expected gamma ray diffuse flux in the Galactic region  $25^\circ < l < 100^\circ$  and  $|b| < 5^\circ$ , compared with the Tibet AS $\gamma$  array data above 100 TeV, the ARGO-YBJ data in the TeV region and a measurement by Fermi at 12 GeV.

The Tibet data are closer to predictions that include the CR hardening, but it is difficult to draw a firm conclusion. The errors on the flux measured by the Tibet array are comparable in size with the differences among predictions. Uncertainties on the CR composition at the knee are still large: a higher proton flux could produce the observed high gamma ray flux as well.

More accurate measurements in different longitudinal bands would be necessary to verify if the high Tibet array flux is a consequence of a lighter elemental composition, or is due to the CR spectral hardening assumed by M2, since in the latter case the enhancement would be present in the region of the Galactic center and absent in the anticenter region.

### 3. Galactic and extragalactic cosmic rays

It is generally assumed that above a “transition energy”  $E^*$  the CR spectrum starts to be dominated by the contribution of extragalactic particles. The identification of the transition energy, and the separation of Galactic and extragalactic components in the CR flux is obviously a problem of fundamental importance for CR astrophysics, and its solution has broad and profound implications.

Several models assume that the Galactic to extragalactic transition corresponds to the spectral feature at  $E \simeq 5 \times 10^{18}$  eV known as the “ankle”. In [2] we adopted for the CR spectrum the model Gaisser-Stanev-Tilav (GST-H3a), constructed using this assumption. In this model the CR spectrum is described as formed by three populations of sources, that generate power law spectra with rigidity dependent exponential cutoffs. Two populations (with proton cutoffs at  $4 \times 10^{15}$  eV and  $3 \times 10^{16}$  eV respectively) are considered of Galactic origin, while the third population (with a higher proton cutoff at  $2 \times 10^{18}$  eV) is considered as extragalactic and emerges as dominant at the ankle.

Several authors have discussed models where the Galactic to extragalactic transition is at the “second Knee”. Two (very similar models) of this type are those developed by Abu-Zayyad et al. [14] and by Mollerach and Roulet (MR) [15]. In these models the CR Galactic component is described as an ensemble of rigidity dependent (gradually) broken power laws, with a result that is numerically very similar to the GST fit for  $E \lesssim 10^{15.5}$  eV. The extragalactic component, in the model of Abu-Zayyad et al. [14] is described with the expression:  $\phi_{\text{extra}}(E) = K E^{-\gamma} \exp[-(E_{\text{cut}}/E)^\beta]$  that is a power law with a low energy exponential cutoff. In the Mollerach and Roulet (MR) model [15] the cutoff has the form  $1/\cosh[(E_{\text{cut}}/E)^\beta]$  that has a very similar (but not identical) shape. The extragalactic component emerges very rapidly for  $E \gtrsim E_{\text{cut}}$  forming the spectral hardening visible at  $E \simeq 2 \times 10^{16}$  eV, and becomes dominant for  $E \gtrsim 10^{17}$  eV (above the so called “second Knee”).

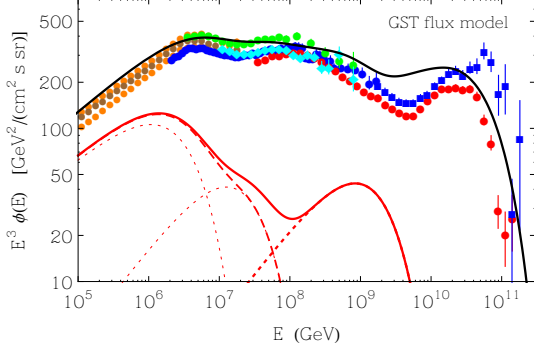


**Figure 7:** The points are measurements of the all-particle CR spectrum. The solid lines are the all-particle (black) and all-nucleon (red) spectra of the GST model [10]. The dashed curves represent the three population of sources, the highest in energy is the extragalactic one.

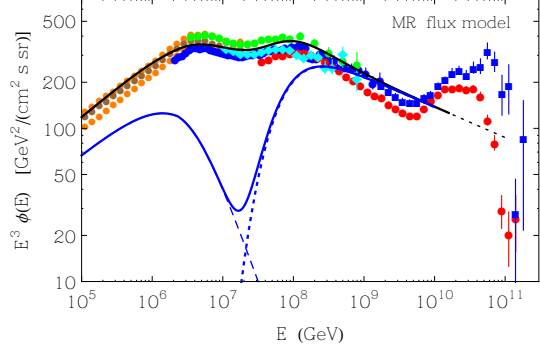


**Figure 8:** The points are as in Fig. 7. The solid lines are the all-particle (black) and all-nucleon (blue) spectra of the MR model [15]. The separate contributions of Galactic and extragalactic particles to the all-nucleon flux are also shown.

The GST and MR models for the CR all-particle and all-nucleon spectra at the Earth are shown in Fig. 7 and 8 together with measurements of the all-particle spectra. Since the MR model is constructed to describe CRs above the knee, we use the GST model to derive the all-nucleon spectra for nucleon energy  $E_0 < 3$  PeV in both cases.

To compute the diffuse  $\gamma$ -ray and  $\nu$  fluxes we have assumed that Galactic CRs have the same spectral shape in all the Galaxy and a density decreasing with  $r$  (the distance from the Galactic center) as described in the previous section for the model M1, while the extragalactic component is homogeneous in space.

The angle integrated  $\gamma$ -ray flux and the flux of  $\nu$ -induced muons (calculated taking into account the effects of flavor oscillations) are shown in Fig. 9 and 10. The contributions of extragalactic CR particles are also shown. It can be seen that the predictions of the two models are equal for  $E_\gamma \lesssim 3$  PeV (and  $E_\mu \lesssim 0.3$  PeV), while at higher energy the MR predictions (assuming a proton extragalactic component) is higher.

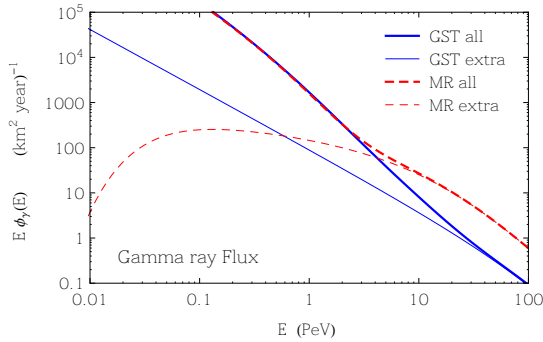


**Figure 9:** Angle integrated diffuse  $\gamma$ -ray flux calculated using the GST and MR models. The contributions generated by extragalactic CRs are also shown.

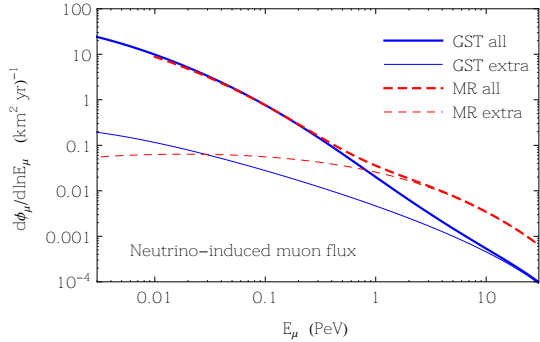


**Figure 10:** Muon flux generated by the Galactic diffuse  $\nu$  flux, calculated using the GST and MR models. The contributions of extragalactic CRs are also shown.

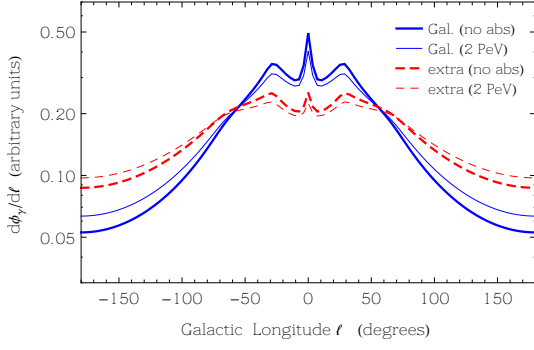


**Figure 11:** Shape of the Galactic longitude distributions of the diffuse  $\gamma$ -ray flux integrated in the latitude range  $|b| \leq 5^\circ$ . The curve with no absorption refer to neutrinos or low energy gamma rays. The calculations assume Galactic and extragalactic energy independent CR space distributions.

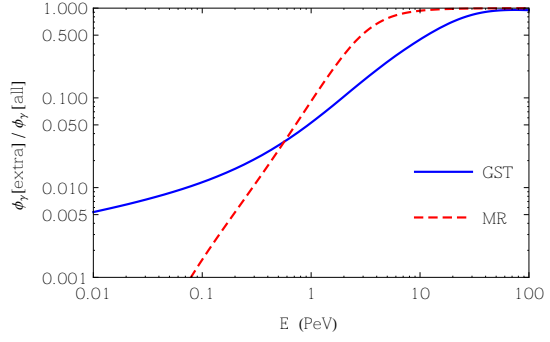


**Figure 12:** Fraction of the diffuse gamma ray flux generated by the extragalactic component for the GST and MR model.

Perhaps the most interesting problem is the identification of an extragalactic component. Information on this can be obtained from the angular distribution of the diffuse fluxes. This is illustrated in Fig. 11, that shows the shape of Galactic longitude distributions of the diffuse gamma ray and neutrinos fluxes after integration in the Galactic latitude range  $|b| < 5^\circ$ . The thick curves show the distributions for a non-absorbed emission (valid for low energy  $\gamma$ -rays and neutrinos) for a Galactic (solid) and extragalactic (dashed) distributions. As it is intuitive, for the component generated by extragalactic CRs (that are modeled with a flat space distributions) the ratio of the fluxes toward the center and anti-center of the Galaxy is smaller than for the component generated by Galactic CRs (that have a density gradient). The effects of absorption for gamma rays (that are largest for  $E_\gamma \sim 2$  PeV, that are shown as thinner lines in Fig. 11) change the shape of the longitude distribution, reducing the center/anti-center ratio, but the difference between the Galactic

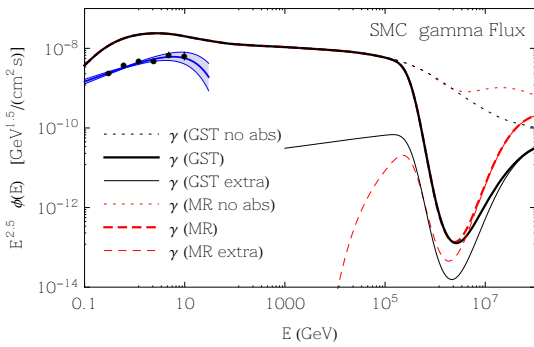


**Figure 13:** Gamma ray flux from the SMC assuming that it contains the same CR density as the local one (and described with the GST and MR models). The extragalactic components are also shown. The points and shaded area show the  $\gamma$ -ray flux from the SMC measured by Fermi.

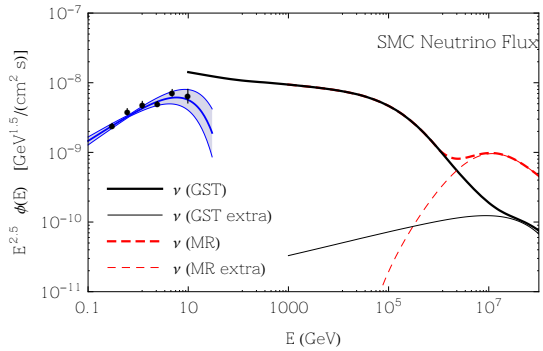


**Figure 14:** The neutrino flux from SMC, under the same assumptions of Fig. 13.

and extragalactic prediction remains significant.

The predictions of the observable angular distributions of the diffuse  $\gamma$ -ray and  $\nu$  fluxes are determined by the relative importance of the contributions of Galactic and extragalactic CR's. Fig. 12 shows the fraction of the diffuse  $\gamma$ -ray flux due to extragalactic CRs as a function of  $E_\gamma$  for the GST and MR models. One can see that at 1 PeV, the contribution of extragalactic CRs is of order 5% (9%) for the GST (MR) model. At an energy of 10 PeV the extragalactic contribution grows to 44% for GST and more than 90% for MR. These estimates suggest that it is important to discuss in depth the problem of the space distribution of Galactic and extragalactic CR's.

Establishing that a component of the CRs has a flat space distribution in a significant part of the Milky Way would suggest an extragalactic origin, but this result could also have alternative explanations. Measuring the CR density in the Magellanic clouds would be a simple extension of the argument first developed by Ginzburg. Prediction for the very high energy  $\gamma$ -ray and  $\nu$  fluxes from the Small Magellanic clouds are shown in Fig. 13. The experimental verification of predictions based on the assumption that the SMC contain an extragalactic component equal to the one estimated at the Earth requires detectors of higher sensitivity than what are available today, but could be a goal for future studies.

## References

- [1] M. Ackermann *et al.* [Fermi-LAT], *Astrophys. J.* **750**, 3 (2012) [arXiv:1202.4039 [astro-ph.HE]].
- [2] P. Lipari and S. Vernetto, *Phys. Rev. D* **98**, no.4, 043003 (2018). [arXiv:1804.10116 [astro-ph.HE]].
- [3] D. Gaggero, A. Urbano, M. Valli and P. Ullio, *Phys. Rev. D* **91**, no. 8, 083012 (2015)
- [4] R. Yang, F. Aharonian and C. Evoli, *Phys. Rev. D* **93**, no. 12, 123007 (2016) [arXiv:1602.04710 [astro-ph.HE]].
- [5] M. Amenomori *et al.* [Tibet AS $\gamma$ ], *Phys. Rev. Lett.* **126**, no.14, 141101 (2021)
- [6] S. Vernetto and P. Lipari, *Phys. Rev. D* **94**, no.6, 063009 (2016). [arXiv:1608.01587 [astro-ph.HE]].
- [7] M. G. Aartsen *et al.* [IceCube-IceTop], *Phys. Rev. D* **100**, no.8, 082002 (2019) [arXiv:1906.04317 [astro-ph.HE]].
- [8] W.D. Aper *et al.* [Kascade-Grande], *Astroparticle Physics* **47**, 54 (2013)
- [9] B. Bartoli *et al.* [ARGO-YBJ], *Phys.Rev.D* **92**, 092005 (2015)
- [10] T. K. Gaisser, T. Stanev and S. Tilav, *Front. Phys. (Beijing)* **8**, 748-758 (2013) [arXiv:1303.3565 [astro-ph.HE]].
- [11] P. Lipari, S. Vernetto, *Astropart.Phys.*, **120**, 102441 (2020) [arXiv:1911.01311 [astro-ph.HE]].
- [12] B. Bartoli *et al.* [ARGO-YBJ], *Astrophys. J.* **806**, 20 [arXiv:1507.06758 [astro-ph.IM]].
- [13] F. Acero *et al.* [Fermi-LAT Collaboration], *Astrophys. J. Suppl.* **223**, no. 2, 26 (2016)
- [14] T. Abu-Zayyad *et al.*, arXiv:1803.07052 [astro-ph.HE].
- [15] S. Mollerach and E. Roulet, *JCAP* **1903**, 017 (2019) [arXiv:1812.04026 [astro-ph.HE]].